Andrzej JANKOWSKI

Polish Academy of Sciences —
Institute of Oceanology in Sopot

Oceanologia, 16 (1983)
PL ISSN 0078-3234

AN H-N MODEL FOR THE CALCULATION OF STEADY WIND- AND DENSITY-DRIVEN CIRCULATION IN THE BALTIC SEA PART II. DENSITY-DRIVEN CIRCULATION IN THE SUMMER SEASON

Contents: 1. Introduction, 2. Equations and boundary conditions, 3. Physical parameters and generating forces, 4. Results of calculations, 5. The role of water density in the formation of circulation in the Baltic Sea, 6. Verification of numerical calculations, 7. Conclusions; Streszczenie; References.

1. INTRODUCTION

Characteristic of the circulation generated by spatially heterogeneous sea water density field is a seasonable variability due to the changes in the structure of the water density field which does not undergo such rapid variations as does the wind velocity field. Heterogeneity and the principal features of the spatial structure of the density field in the Baltic Sea are formed under the influence of wated exchange with the North Sea occurring through the Danish Straits, the inflow of solar energy and a substantial inflow of river waters [17].

The diversified topography of the Baltic sea bed together with relatively small depths (a mean depth of about 55 m) mean that the application of the dynamic method [10] to estimate the currents presents certain difficulties.

Attempts to apply this method in the Baltic basin were taken up [18]. The problems related to the application of the classic method to assess currents in a heterogeneous sea can be overcome by the employment of mathematical models of the circulation. Such models were presented for the Baltic Sea in papers by Kowalik and Taranowska [10], Sarkisyan et al. [15], Kowalik and Staśkiewicz [9]. In the two latter papers, the global wind- and density-driven circulation in the summer season (August) was considered, being calculated basing on the method by Sarkisyan [14]. In the paper by Kowalik and Taranowska [10] only density-driven circulation for the same period of the year was discussed.

The present paper refers to the above-mentioned model investiga-

tions, constituting the second part of paper [7] which deals with the hydrodynamic-numerical (H-N) model for the calculation of steady wind- and density-driven circulation in the Baltic Sea. As compared with previous models [9, 10, 15], the whole of the Baltic Sea together with its main gulfs, i.e., the Gulf of Bothnia, Gulf of Finland and Gulf of Riga, will be the subject of our considerations. A method of parametrization of the vertical temperature and water salinity distributions [8] was used to work out the water density field. The method enables the assessment of currents at any depth in the water body.

In this paper we shall discuss the results of the calculations of mass tranport, sea level and currents for August, which is a characteristic month in the Baltic. The essential part of the results will concern purely density-driven circulation. Global currents, i.e., the wind- and density-driven, will be discussed when considering the vertical structure of currents and comparing the results of the calculations with those of in situ observations. In a qualitative assessment of the results of model calculations we shall also apply the spatial distributions of hydrological parameters of the Baltic Sea.

2. EQUATIONS AND BOUNDARY CONDITIONS

The H-N model for the calculation of circulation is based on the system of equations for mass transport and sea level [7]:

$$\frac{\partial M_x}{\partial t} - \Omega M_y = \tau_x - RM_x - \varrho_0 gH \frac{\partial \zeta}{\partial x} - H \frac{\partial p_a}{\partial x} - S_x \tag{1}$$

$$\frac{\partial M_y}{\partial t} + \Omega M_x = \tau_y - RM_y - \varrho_0 gH \frac{\partial \zeta}{\partial y} - H \frac{\partial p_a}{\partial y} - S_y \tag{2}$$

$$\frac{\partial \zeta}{\partial t} = -\frac{1}{\varrho_0}\left(\frac{\partial M_x}{\partial x} + \frac{\partial M_y}{\partial y}\right) \tag{3}$$

where:

$$S_x = g \int_{-H}^{0} \int_{Z}^{0} \frac{\partial \varrho}{\partial x} d\eta dz \tag{4}$$

$$S_y = g \int_{-H}^{0} \int_{Z}^{0} \frac{\partial \varrho}{\partial y} d\eta dz \tag{5}$$

The equilibrium state is described by the initial conditions:

$$M_x = M_y = \zeta = 0 \qquad \text{for} \qquad t = 0 \tag{6}$$

Boundary conditions for the mass transport component normal to the contour L of the coast line, in the case of a closed basin can be written as:

$$M_n|_L = 0 \tag{7}$$

In the H-N model, the horizontal components, u and v, of the current are calculated by means of the analytical expression [7]:

$$D = u + iv = \frac{\tau}{\varrho_0 p_1 A} \frac{\operatorname{ch} p_1 (H+z)}{\operatorname{sh} p_1 H} + \left[-\frac{RM}{\varrho_0 p_1 A} + \right.$$

$$\left. + B_1(x,y,-H)\exp(-p_1 H) - B_2(x,y,-H)\exp(p_1 H) \right] \frac{\operatorname{ch} p_1 z}{\operatorname{sh} p_1 H} +$$

$$+ B_1(x,y,z)\exp(p_1 z) + B_2(x,y,z)\exp(-p_1 z) + C_1(p_a, \zeta) \tag{8}$$

where:

$$C_1(p_a, \zeta) = \frac{1}{\varrho_0 \Omega} i \left(\frac{\partial p_a}{\partial x} + i \frac{\partial p_a}{\partial y} \right) + \frac{g}{\Omega} i \left(\frac{\partial \zeta}{\partial x} + i \frac{\partial \zeta}{\partial y} \right) \tag{9}$$

$$B_1(x,y,z) = \frac{1}{2p_1} \int_0^z C(x,y,\eta)\exp(-p_1 \eta)\, d\eta \tag{10}$$

$$B_2(x,y,z) = -\frac{1}{2p_1} \int_0^z C(x,y,\eta)\exp(p_1 \eta)\, d\eta \tag{11}$$

$$C(x,y,z) = \frac{g}{\varrho_0 A} \int_z^0 \left(\frac{\partial \varrho}{\partial x} + i \frac{\partial \varrho}{\partial y} \right) d\eta \tag{12}$$

$$p_1 = \sqrt{\frac{\Omega}{A} i} \quad ; \quad \tau = \tau_x + i\tau_y \qquad M = M_x + i M_y \tag{13}$$

The above equations are written in a rectangular coordinate system the origin of which lies on the free sea surface, the x-axis is directed to the east, y-axis to the west and the z-axis — vertically upwards. The denotations used in equations (1—13) represent the following parameters:

p_a — atmospheric pressure at the sea surface,
ξ — sea level (deviation from the equilibrium state),
H — sea depth,
A — coefficient of the vertical turbulent exchange of momentum,
R — friction coefficient at the sea bottom,
Ω — the Coriolis parameter ($\Omega = \text{const} = 1{,}2368 \times 10^{-4} s^{-1}$),
g — gravity ($g = 980.777$ cm s^{-2}),
ϱ_o — mean water density ($\varrho_o = \text{const}$),
ϱ — water density anomaly,
u, v — horizontal components of current velocity,
τ_x, τ_y — components of tangent wind stress,

$$M_x = \int_{-H}^{0} \varrho_o u \, dz$$

$$M_y = \int_{-H}^{0} \varrho v \, dz$$

— mass transport components along the x- and y-axis, respectively.

3. PHYSICAL PARAMETERS AND GENERATING FORCES

In the present paper we shall consider density-driven circulation, whereas global wind- and density-driven currents will be taken into account during the verification of the model calculations only. The system of equations (1—3) and (8) is linear which permits assessment of mass transports, sea level and current separately for the case of the wind-driven generating forces and those created by the spatial heterogeneity of the water density field. The global water circulation will be the sum of the circulations generated by the above-mentioned factors. Wind-driven circulation in the homogeneous Baltic for the summer season (August) was discussed by the author in paper [7]. We shall now consider currents generated by the heterogeneity of the water density field in the Baltic Sea in August.

The wind field which is necessary to assess the friction coefficients R at the bottom, as well as he method of calculating these parameters are given in paper [7]. The water density field was prepared by modelling the vertical structures of temperature (T) and salinity (S) [4, 19].

Two- or three-layer structure of the T and S fields is characteristic of the Baltic Sea waters [17]. We approximate vertical distributions of temperature and salinity in each layer by means of polynominals with z-variable:

$$f(z) = \sum_{n=1}^{r} d_n z^{n-1} \qquad r = 2,3,4 \tag{14}$$

where:

$f(z)$ — denotes water temperature or salinity.

We shall assess the d_n coefficients using the experimental data for temperature and salinity [1, 11] and the continuity of function $f(z)$ and its derivatives at the interfaces of individual layers. The Mamaev formula [12] was used as a state function:

$$\varrho = C_1 + C_2T + C_3T^2 + C_4S + C_5TS \tag{15}$$

where coefficients C_i are constant.

A more detailed discussion on the method of approximating the vertical distributions of water temperature and salinity and the results of calculations of T, S and ϱ are presented in paper [8]. The water density field for August obtained there will be used to calculate integrals in equations (1), (2) and (8).

4. RESULTS OF CALCULATIONS

Numerical calculations were performed applying the H-N differential scheme [5, 6] and assuming the spatial step of the numerical grid to be $h=5$ Mm and the time step $\Delta t=120$ s. For the type of circulation considered (purely density-driven circulation), $\tau_x=\tau_y=0$ and $p_a=$const in equations (1—3). Integrating equations (1—3) in relation to time with the initial and boundary conditions (6), (7) and time constant generating forces, we obtain a steady state after a certain period. Exemplary oscillations of the sea level during calculations at a given point in the Baltic are shown in Fig. 1. The results of the calculations of mass transports, sea level and bottom and surface currents are illustrated in Figs. 2—5.

Characteristic of the mass transport field (Fig. 2) is a complex system of gyres. Strong cyclonic gyres occur in Bornholm Deep, in the central part of the southern Baltic, in the southern area of the Gulf of Bothnia and in the Gulf of Riga. Gyratory counter structures can be observed in Gdańsk, Gotland and Landsort Deeps. Maximum values of mass transport of the order of 1.67×10^5 g cm^{-1}s^{-1} can be found in

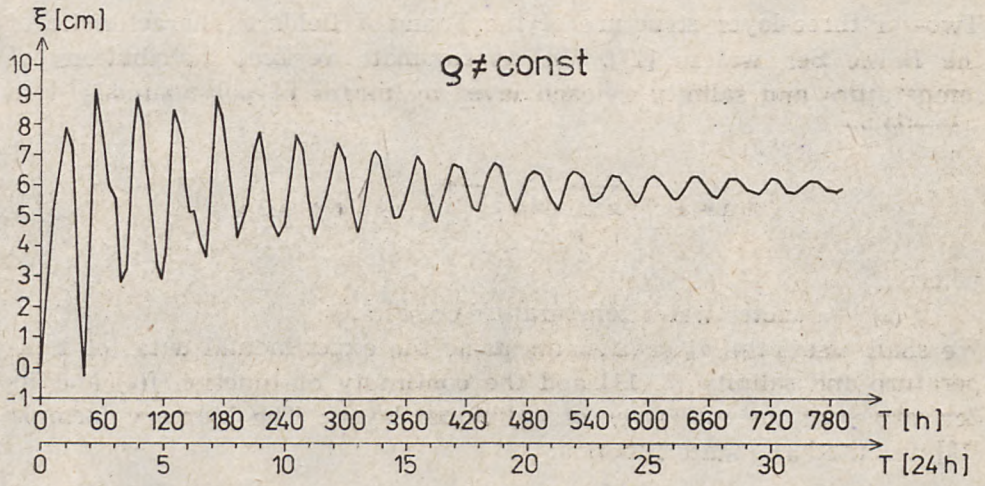

Fig. 1. Sea level oscillations during computations at a given point in the Baltic (density-driven circulation). Steady state is attained after 780 hours

Rys. 1. Oscylacje poziomu morza w czasie obliczeń numerycznych w wybranym punkcie Bałtyku (przepływy gęstościowe). Stan ustalony następuje po upływie 780 godz.

Gotland Deep. The gyre distribution in the mass transport vector field is similar to the configuration of isolines of the sea level field (Fig. 3).

The values of the ordinates of the free sea surface fluctuate from −8.7 cm in the vicinity of the Danish Straits to 6.8 cm in the Gulf of Finland. The highest density of the sea level isolines can be observed in the southern Baltic, particularly in Bornholm Deep.

The field of surface currents (Fig. 4) exhibits a distribution of the current velocity vectors (gradient circulation) similar to the configuration of the sea level isolines. Gyres occurring in the field of surface currents are of a cyclonic character. Maximum current velocities occur in Bornholm Deep, attaining values of the order of 16.0 cm s^{-1}. The field of bottom currents is slightly different (Fig. 5). Cyclonic gyres occur over a considerable area of the Baltic. In Gotland and Landsort Deeps, however, strong anticyclonic gyres can be observed. Sea bottom currents attain higher velocities than on the surface, the maximum value reaching 17.4 cm s^{-1}.

5. THE ROLE OF WATER DENSITY IN THE FORMATION OF CIRCULATION IN THE BALTIC SEA

The fields of mass transport, sea level and currents calculated are closely related to the water density field at the bottom (Fig. 6), as well as to the depth field of the Baltic (see [7]). These conclusions are confirmed

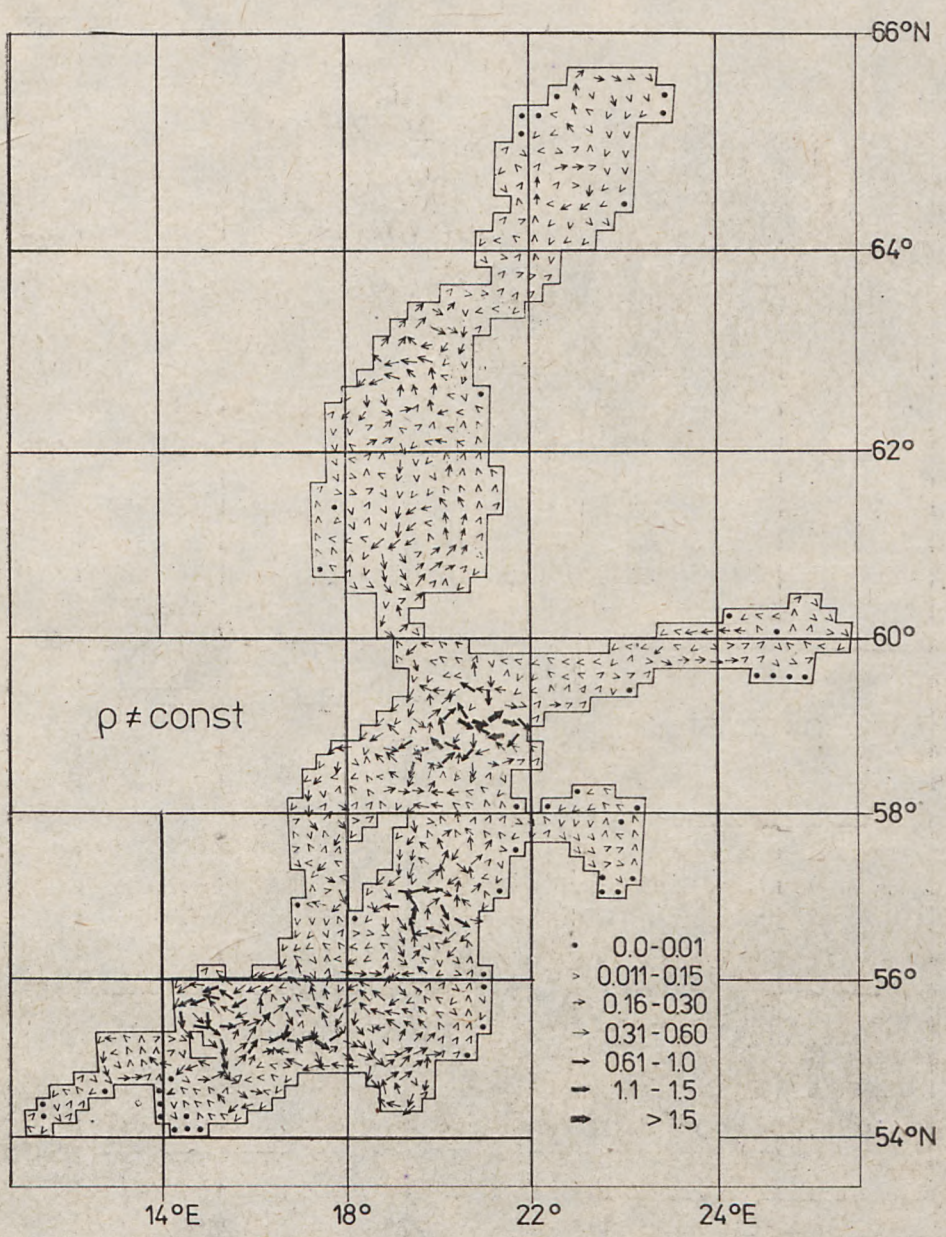

Fig. 2. Mass transport field [10^5 g cm^{-1} s^{-1}] in the Baltic for density-driven circulation

Rys. 2. Pole wydatków masowych [10^5 g cm^{-1} s^{-1}] w Bałtyku dla przepływów gęstościowych

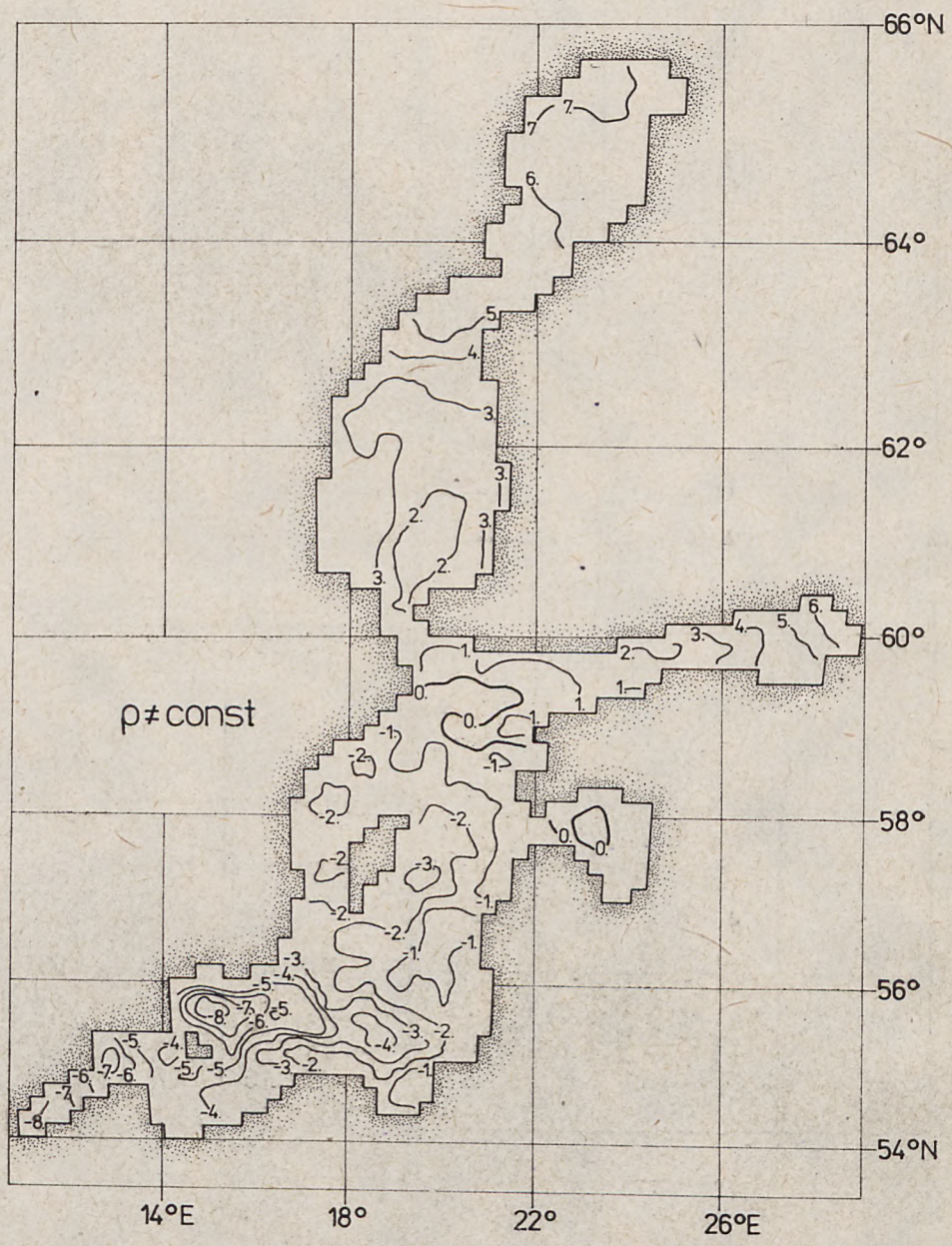

Fig. 3. Sea level field [cm] in the Baltic, for density-driven circulation

Rys. 3. Pole poziomu morza [cm] w Bałtyku dla przepływów gęstościowych

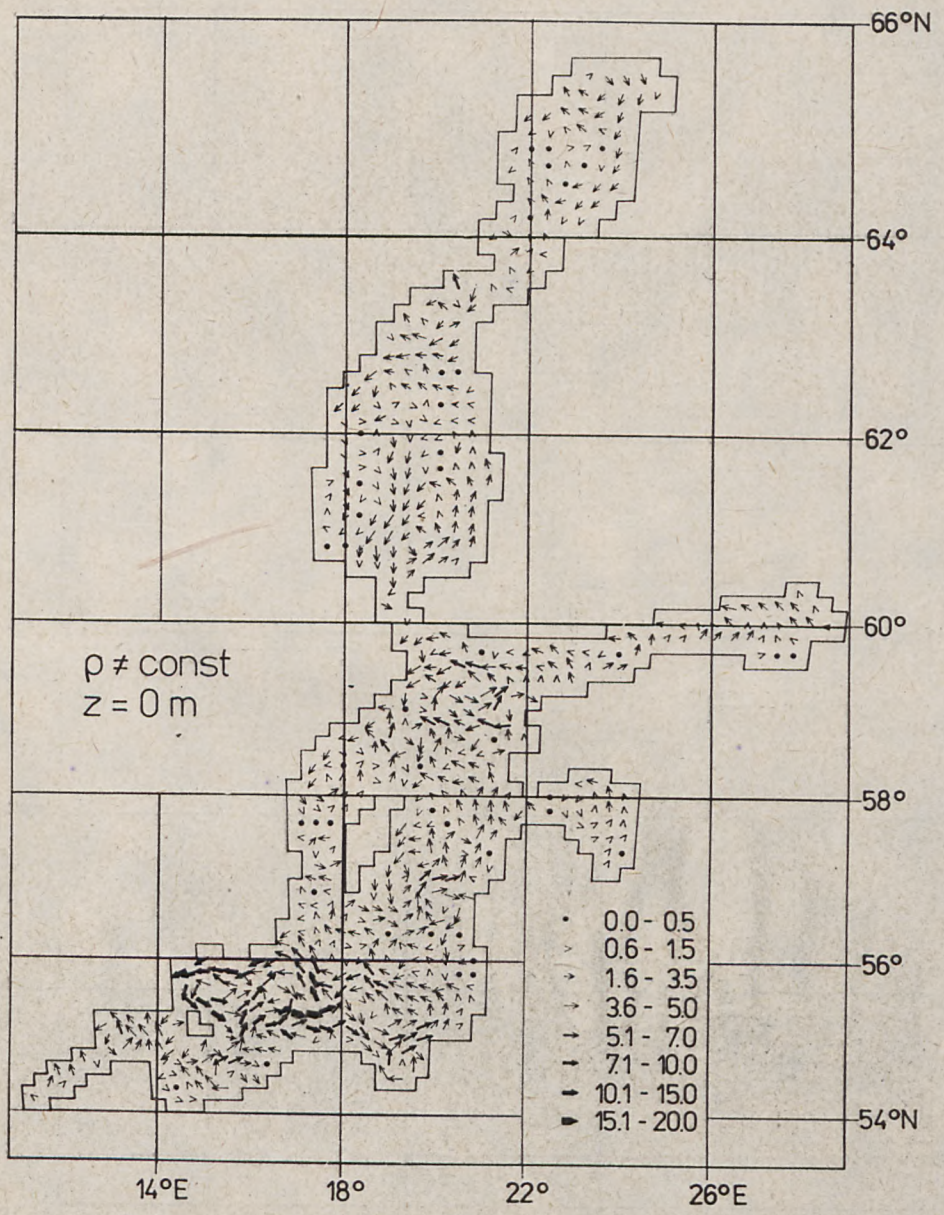

Fig. 4. Surface current field [cm s^{-1}] in the Baltic, for density-driven circulation

Rys. 4. Pole prądów [cm s^{-1}] na powierzchni morza w Bałtyku dla przepływów gęstościowych

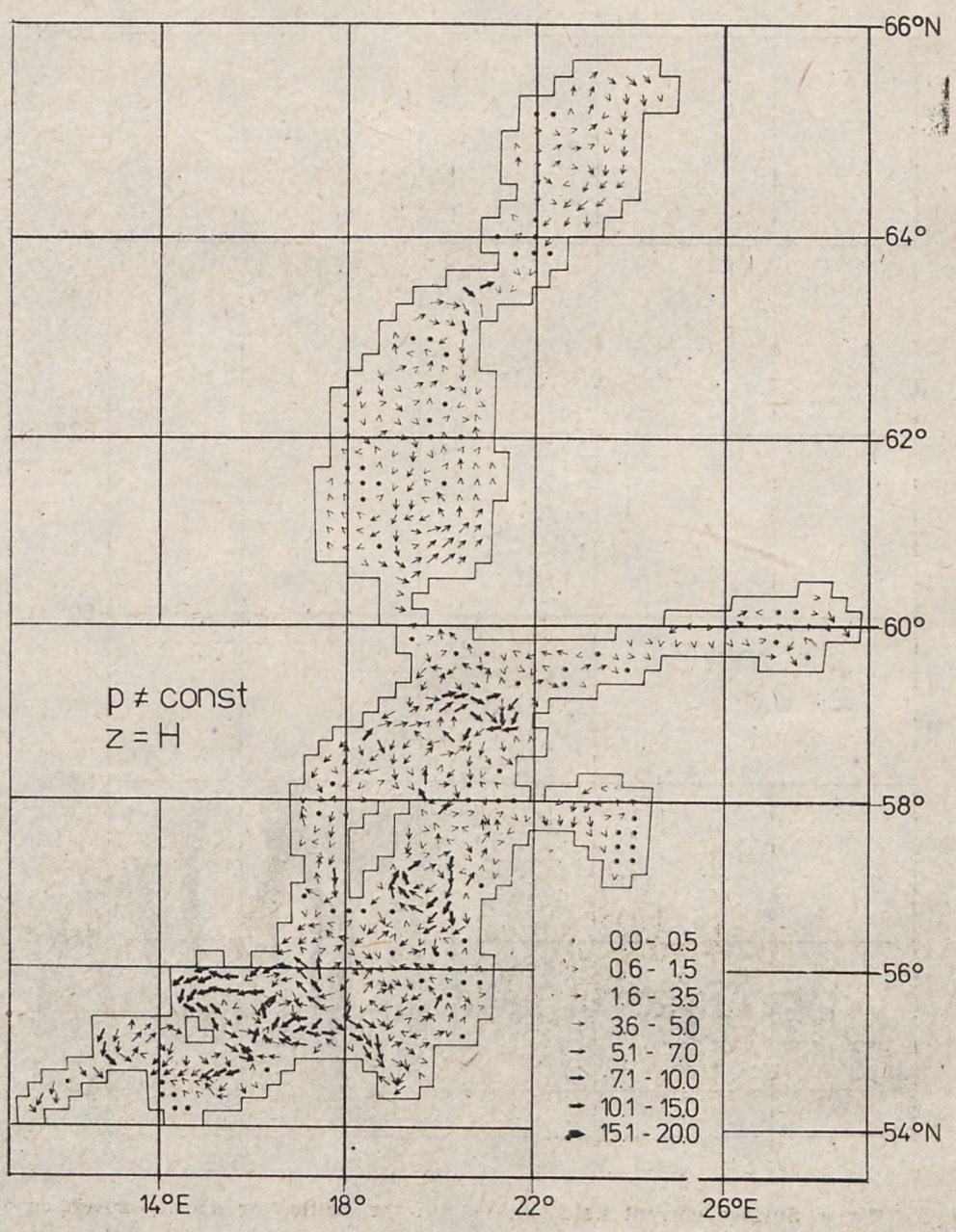

Fig. 5. Bottom current field [cm s^{-1}] in the Baltic, for density-driven circulation

Rys. 5. Pole prądów [cm s^{-1}] na dnie morza w Bałtyku dla przepływów gęstościowych

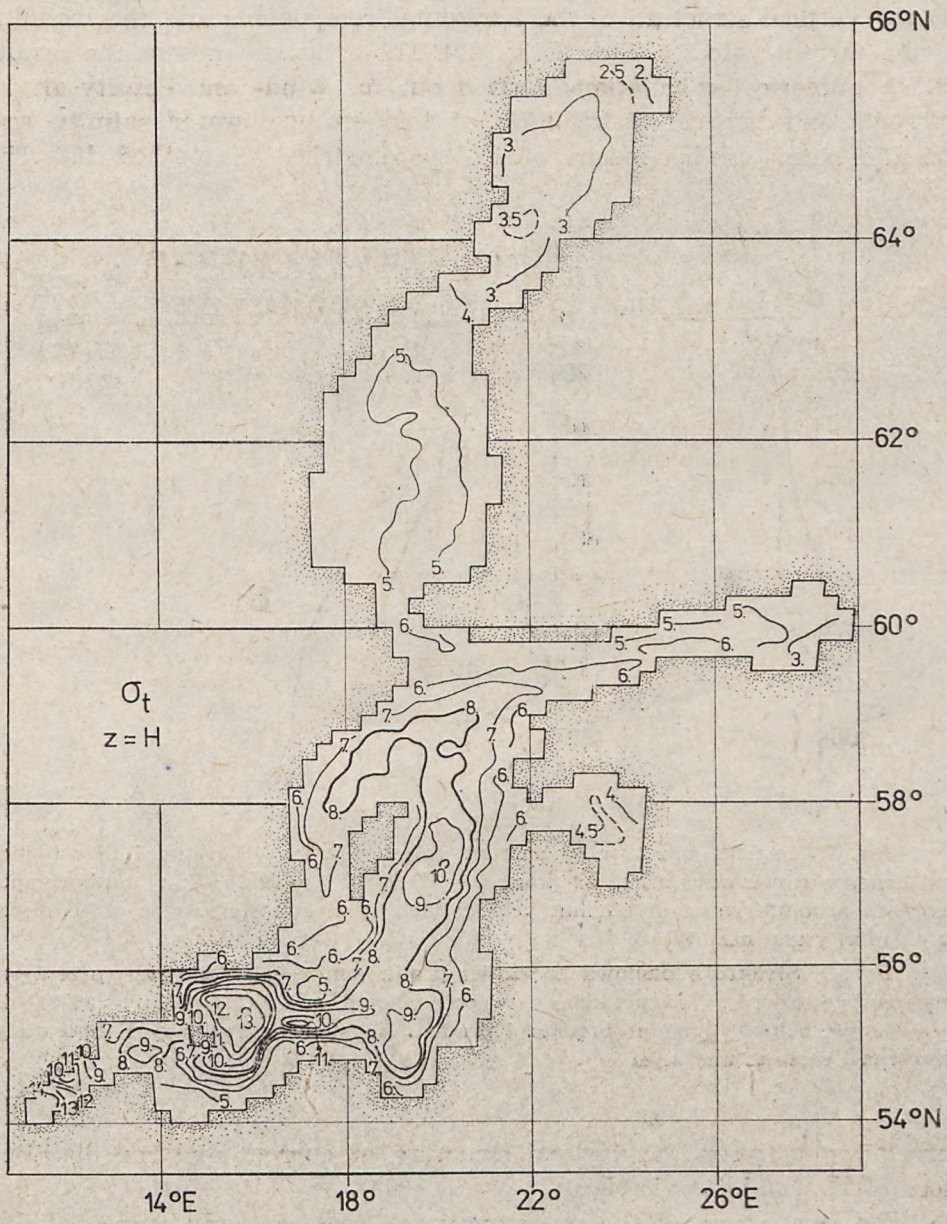

Fig. 6. Water density field σ_t on the Baltic Sea floor, calculated by means of the parametrization method [8]

Rys. 6. Pole gęstości umownej σ_t na dnie morza w Bałtyku obiczone metodą parametryzacji [8]

by the vertical structure of the horizontal components and the modulus of the current velocity (Figs. 7, 8a, 8b). These figures present the results of the numerical calculations carried out for wind- and density-driven currents and vertical distribution of temperature, water salinity and density estimated by means of the parametrization method [8]. The

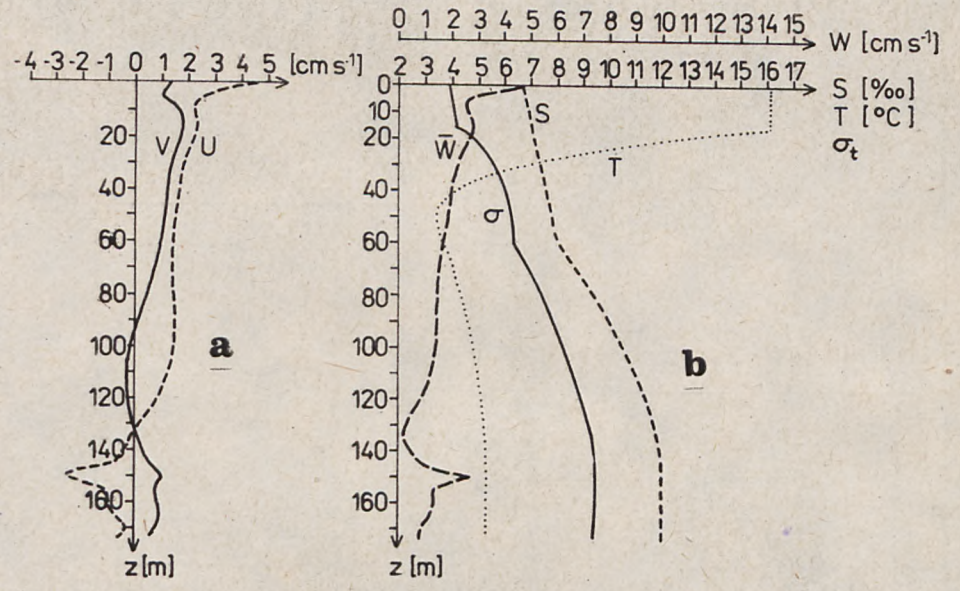

Fig. 7. Vertical structure of current velocity [cm s—1] in the Baltic (wind- and density-driven circulation) at point $\varphi = 57°28'$ N, $\lambda = 20°14'$ E: *a*) total components, *b*) absolute value of current velocity and vertical distributions of temperature, salinity and density

Rys. 7. Struktura pionowa prędkości prądu [cm s—1] w Bałtyku (przepływy wiatrowo-gęstościowe) w punkcie o współrzędnych $\varphi = 57°28'$ N, $\lambda = 20°14'$ E: *a*) składowe pełne, *b*) moduł prędkości prądu oraz pionowe rozkłady temperatury, zasolenia i gęstości umownej

correlation between the vertical structure of current and the distributions of T, S and ϱ is visible.

The comparison of the mass transport, sea level and current fields for wind-driven circulation in the homogeneous Baltic [7] with the density-driven fields (Figs. 2, 3, 4) indicated that in the summer season, density-driven circulations influence the formation of water circulation in the Baltic Sea. Their spatial structure results from the interaction between the heterogeneity of the waer density field, particularly in the near-bottom layer, and the sea bed topography. Similar conclusions can be reached from papers by other authors [15, 16, 19].

Taking advantage of the H-N model linearity, the roles played by

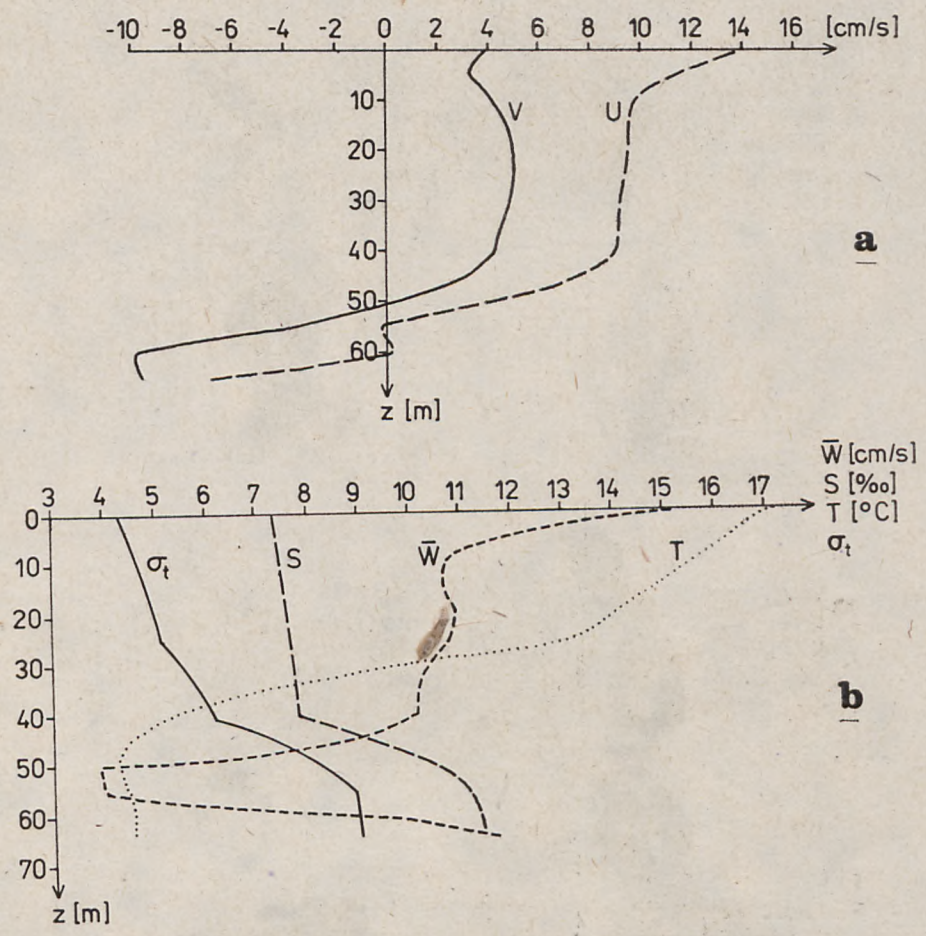

Fig. 8. Vertical structure of current velocity [cm s^{-1}] in the Baltic (wind- and density-driven circulation) at point $\varphi = 55°19'$ N, $\lambda = 16°36'$ E: *a*) total components, *b*) absolute value of current velocity and vertical distribution of temperature, salinity and density

Rys. 8. Struktura pionowa prędkości prądu [cm s^{-1}] w Bałtyku (przepływy wiatrowo-gęstościowe) w punkcie o współrzędnych $\varphi = 55°19'$ N, $\lambda = 16°36'$ E: *a*) składowe pełne, *b*) moduł prędkości prądu oraz pionowe rozkłady temperatury, zasolenia i gęstości umownej

these two factors generating circulation in the Baltic Sea have been assessed separately. The question which appears to be interesting is: at what value of wind velocity can the influence of the heterogeneity of the water density field be omitted when applying the linear model for calculations. To attain this, let us compare the absolute values of sea level and sea surface currents for density- and wind-driven circulations generated by the westerly winds of constant velocity. Fig. 9 shows schematic comparative maps. Analogical considerations can be carried

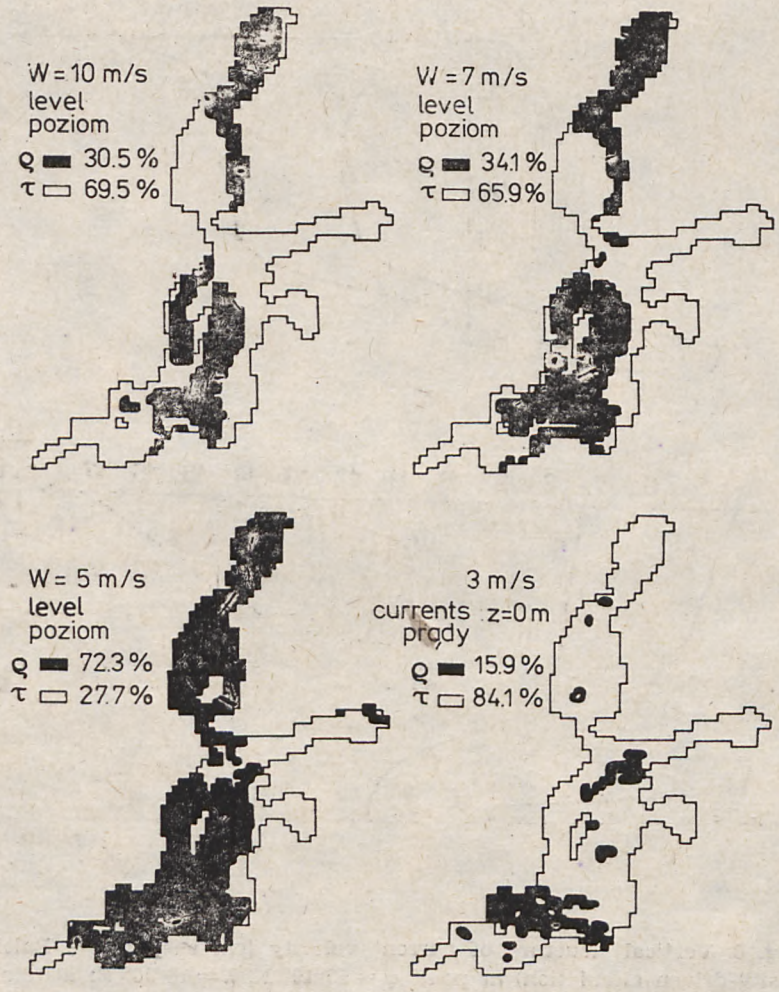

Fig. 9. Schematic charts illustrating the influence of water density and wind upon sea level and surface currents in the Baltic. Darkened patches indicate the predominance of water density

Rys. 9. Schematyczne mapki ilustrujące wpływ gęstości wody i wiatru na poziom morza i prądy na powierzchni Bałtyku. Miejsca zaczernione wskazują na przeważającą rolę gęstości wody

out for the vertical structure of currents (Figs. 10 and 11). Analyzing Figs. 9—11 it can be seen that a predominant role in the greater part of the Baltic is played by winds with velocities of $W_a \sim 7$—10 m s^{-1}. In the case of surface currents, low winds ($W_a \sim 3$ m s^{-1}) also prevail. In the deeper layers of the sea the situation is different. Here, only currents generated by high winds ($W_a \sim 10$ m s^{-1}) have a certain contribution to magnitude of the global current.

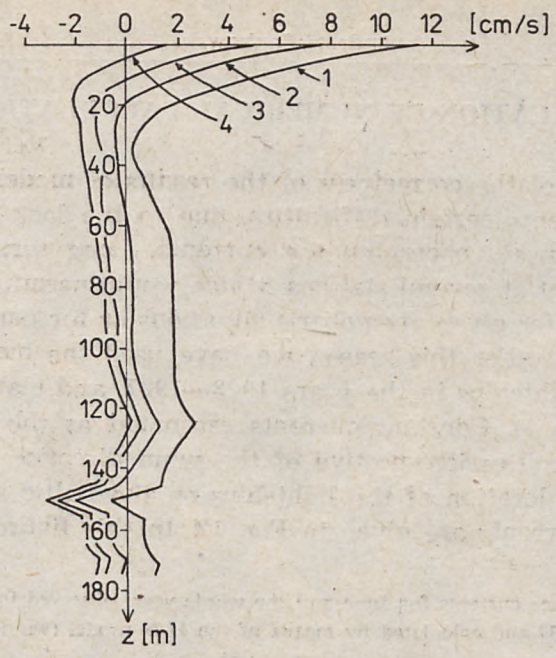

Fig. 10. Differences between the absolute values of density and wind-driven currents (west winds with a constant velocity: *1* — 10 m s^{-1}; *2* — 7 m s^{-1}; *3* — 5 m s^{-1}; *4* — 3 m s^{-1}) as a function of depth at point φ=57°28′ N, λ=20°14′ E. Negative values indicate the predominance of water density

Rys. 10. Różnice pomiędzy modułami prędkości prądów gęstościowych i wiatrowych (wiatry zachodnie o stałej prędkości: *1* — 10 m s^{-1}; *2* — 7 m s^{-1}; *3* — 5 m s^{-1}; *4* — 3 m s^{-1}) w funkcji głębokości w punkcie o współrzędnych φ = = 57°28′ N, λ = 20°14′ E. Ujemne wartości wskazują na przewagę gęstości wody.

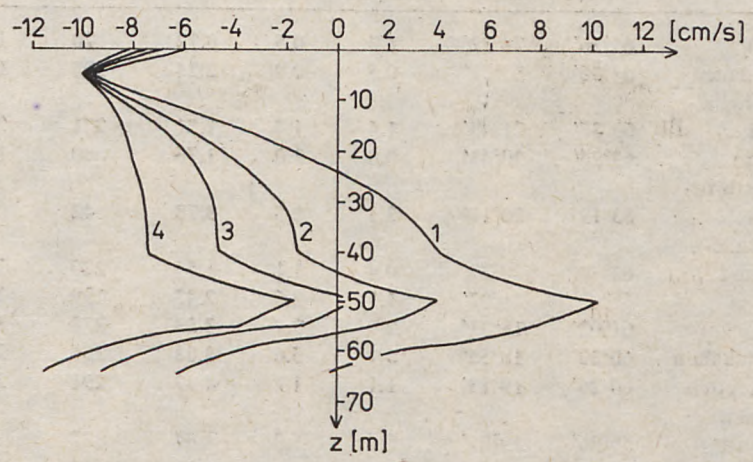

Fig. 11. Differences between the absolute values of density and wind-driven currents (west winds with a constant velocity: *1* — 10 m s^{-1}; *2* — 7 m s^{-1}; *3* — 5 m s^{-1}; *4* — 3 m s^{-1}) as a function of depth at point φ = 55°19′ N, λ = =16°36′ E. Negative values indicate the predominance of water density

Rys. 11. Różnice pomiędzy modułami prędkości prądów gęstościowych i wiatrowych (wiatry zachodnie o stałej prędkości: *1* — 10 m s^{-1}; *2* — 7 m s^{-1}; *3* — 5 m s^{-1}; *4* — 3 m s^{-1}) w funkcji głębokości w punkcie o współrzędnych φ = 55°19′ N, λ = 16°36′ E. Ujemne wartości wskazują na przewagę gęstości wody

6. VERIFICATION OF NUMERICAL CALCULATIONS

The assessment of the correctness of the results of modelling the steady circulation presents certain difficulties, due to the lack of suitable observational material concerning the currents. Long series of measurements carried out at several stations, which would permit the assessment of current field for given anemobaric situations or for particular seasons, are indispensable. For this reason we have used the material collected from Finnish lightships in the years 1923—1927, and elaborated by Palmen [13] (Table 1). Constant currents estimated as the vector sum of the current velocities irrespective of the wind direction [18], are given in Table 2. The location of the lightships on the Baltic and the graphic image of the currents are given in Fig. 12. In this figure and in Tables

Table 1. Mean surface currents for June and the whole year, observed from lightships in the years 1923–1927 [13] and calculated by means of the H-N model (wind- and density-driven circulation)

Tab. 1. Powierzchniowe prądy średnie dla czerwca i roku na podstawie obserwacji na latarniowcach w latach 1923–1927 [13] oraz obliczone za pomocą modelu H-N (przepływy wiatrowo-gęstościowe)

No.[a] Lp.[a]	Lightship Nazwa latarniowca	Geographic coordinates Współrzędne geograficzne		Current velocity [cm s^{-1}] Prędkość prądu [cm s^{-1}]			Current direction[b] Kierunek prądu[b]		
				June	year	model	June	year	model
		φ (N)	λ (E)	czerwiec	rok	model	czerwiec	rok	model
1	Kemi	65°26′	24°22′	1.0	0.5	0.72	70	107	203.2
2	Nahkianen	64°36′	23°51′	0.5	0.9	2.24	108	103	249.9
3	Helsinghallan	63°37′	21°43′	1.4	1.4	1.81	221	231	345.9
4	Snipan	63°26′	20°43′	0.8	1.0	1.76	80	141	228.7
5	Sydostbrotten	63°19′	20°11′	3.5	2.5	3.78	42	39	73.2
6	Storkallegrund	62°40′	20°39′	0.4	1.1	1.59	220	181	355.6
7	Rauma	61°07′	21°07′	1.1	2.5	2.47	199	205	56.6
8	Finngrundet	61°02′	18°31′	2.9	3.2	3.53	278	301	170.2
9	Grundkallan	60°30′	18°55′	5.1	5.6	3.88	286	283	133.0
10	Storbrotten	60°26′	19°13′	1.1	1.8	4.99	291	333	79.0
11	Svenska Björn	59°36′	19°56′	3.4	5.0	1.04	32	11	110.7
12	Helsinki	59°57′	24°57′	1.2	2.2	1.22	48	86	22.9
13	Kalbadagrund	59°58′	25°36′	0.9	1.3	2.22	97	58	53.9
14	Tallinn	59°43′	24°44′	1.3	3.2	4.24	161	243	105.1
15	Hiiumadal	59°06′	22°12′	3.5	3.8	6.04	223	221	92.5

[a] Numbers denote the positions of the lightships in Fig. 12. – Liczby oznaczają położenie latarniowców na rys. 12.

[b] Direction of current measured clockwise of N. – Kierunek prądu mierzony od N zgodnie z ruchem wskazówek zegara.

Table 2. Constant currents observed from lightship [18] and calculated by means of the H-N model (global wind- and density-driven circulation on the sea surface)

Tab. 2. Prądy stałe obserwowane na latarniowcach [18] i obliczone za pomocą modelu H-N (sumaryczne wiatrowo-gęstościowe na powierzchni morza)

No.[a] Lp.[a]	Lightship Nazwa latarniowca	Geographic coordinates Współrzędne geograficzne		Current velocity [cm s^{-1}] Prędkość prądu [cm s^{-1}]		Current direction[b] Kierunek prądu[b]	
		φ (N)	λ (E)	constant stałe	model	constant stałe	model
10	Storbrotten	62°26′	19°13′	6.9	4.99	312	79.0
11	Svenska Björn	59°36′	19°56′	4.0	1.04	173	110.7
12	Helsinki	59°57′	24°57′	3.1	1.22	90	22.9
15	Hiiumadal	59°06′	22°12′	3.0	6.04	12	92.5
16	Owiszi	57°38′	21°36′	3.9	4.12	32	59.0
17	Libawskij	56°32′	20°56′	4.0	3.33	14	125.7
18	Elansrev	56°07′	16°34′	5.0	6.16	217	237.5
19	Adlergrund	54°50′	14°25′	3.4	2.82	84	129.6

[a] Numbers denote the positions of the lightships in Fig. 12 – Liczby oznaczają położenie latarniowców na rys. 12.
[b] Direction of current measured clockwise of N. – Kierunek prądu mierzony od N zgodnie z ruchem wskazówek zegara.

1 and 2, the values of currents calculated for global circulation are given. The values of velocities are similar. In relation to the measurements, there is a greater discrepancy in the directions of the currents calculated. This is due to the fact that the observational material does not strictly correspond to the thermohaline and anemobaric situations for which the circulation was modelled in the Baltic Sea.

In order to assess the vertical structure of currents, the observation of currents in Gdańsk Deep was undertaken (from 31 July to 12 August 1964) [2]. Fig. 13 shows the results of the measurements of current and water density, model profiles of current velocity, density, temperature and water salinity also being given. In this case, only a qualitative comparison is possible, as the anemobaric situation during the measurements differed significantly from that of the model (strong southwest winds with velocities of the order of 8—12 m s^{-1}). The close correspondence between the experimental and calculated curves indicates that the model applied gives a description of the influence of the density field on the vertical structure of currents.

7. CONCLUSIONS

On completing our considerations on the results of modelling of circulation in the heterogeneous Baltic we shall comment on the application of the results of the calculations. It seems to us that the correlation of

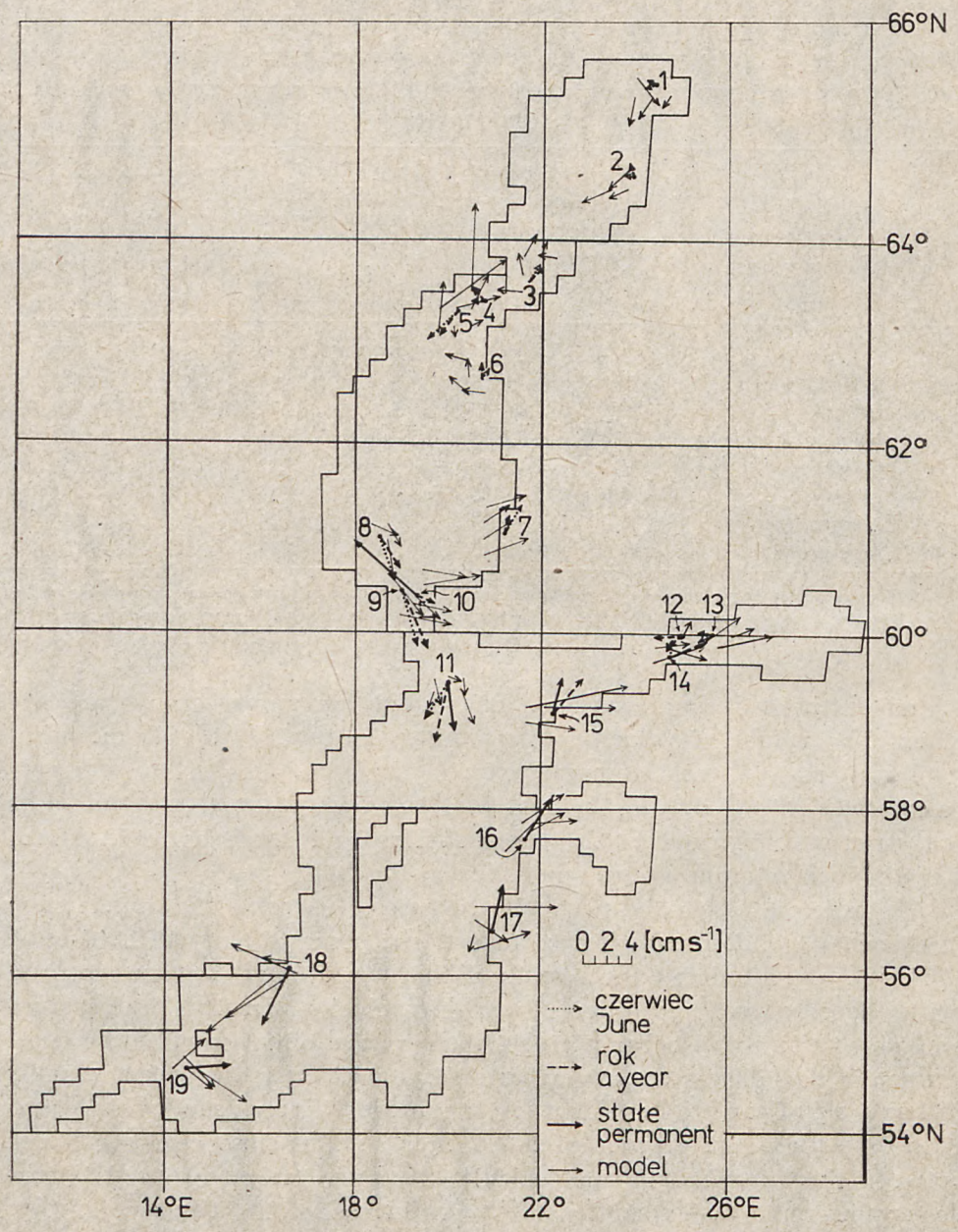

Fig. 12. Comparison between currents calculated for wind- and density-driven circulation and those observed from lightships (mean values for the years 1923—1927 for June and the whole year) [13] and constant currents [18]

Rys. 12. Porównanie prądów obliczonych dla przepływów wiatrowo-gęstościowych z obserwowanymi na latarniowcach (średnie za lata 1923—1927 dla czerwca i roku) [13] oraz prądami stałymi [18]

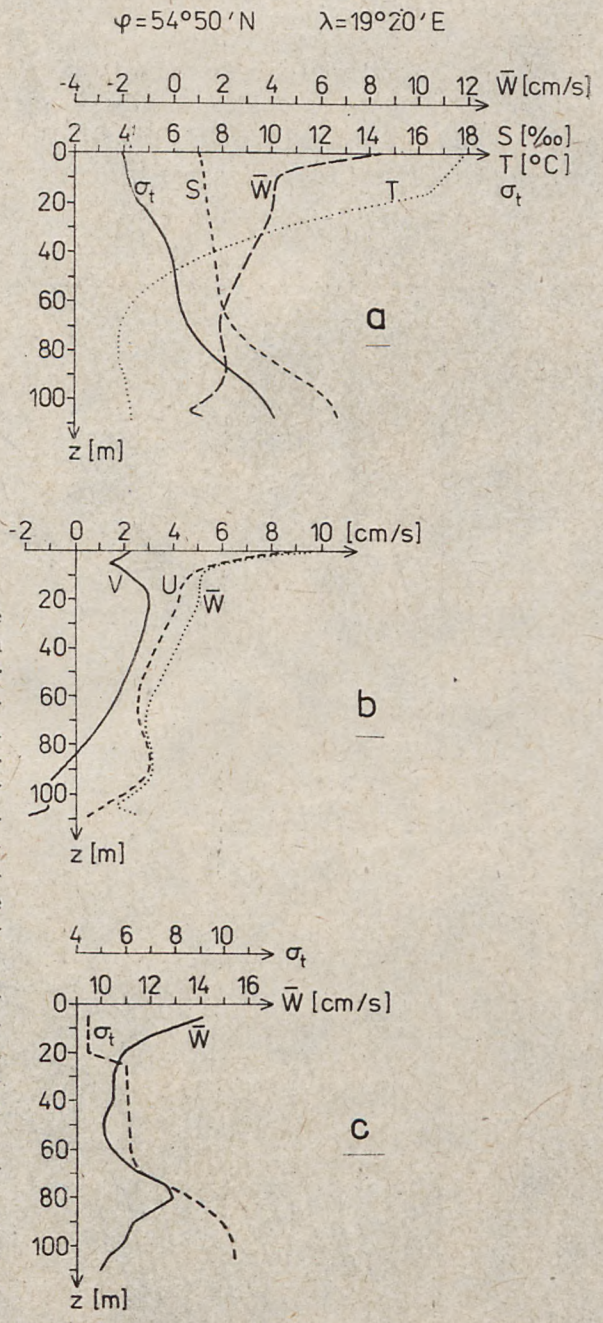

Fig. 13. Comparison of the vertical structure of currents in Gdańsk Deep, calculated for wind- and density-driven circulation and those measured in situ [2]: a) components and absolute value of current velocity — calculations, b) absolute value of current velocity, temperature, salinity and density — calculations, c) absolute value of current velocity and density — measurements

Rys. 13. Porównanie struktury pionowej prądów na Głębi Gdańskiej, obliczonych dla przepływów wiatrowo-gęstościowych i pomierzonych in situ [2]: *a* — składowe i moduł prędkości prądu — obliczenia, *b* — moduł prędkości prądu, temperatura, zasolenie i gęstość umowna — obliczenia, *c* — moduł prędkości prądu i gęstość umowna — pomiary

gyres in the mass transport and current fields with the field of water density and sea bottom configuration, enables the application of the results of the calculations to assess the distribution and spreading of pollution, nutrients or chemical substances. The distribution of oxygen, silicates and phosphates in the near-bottom layer of the Baltic [4] is presented in Figs. 14--16 in order to emphasize the relation between

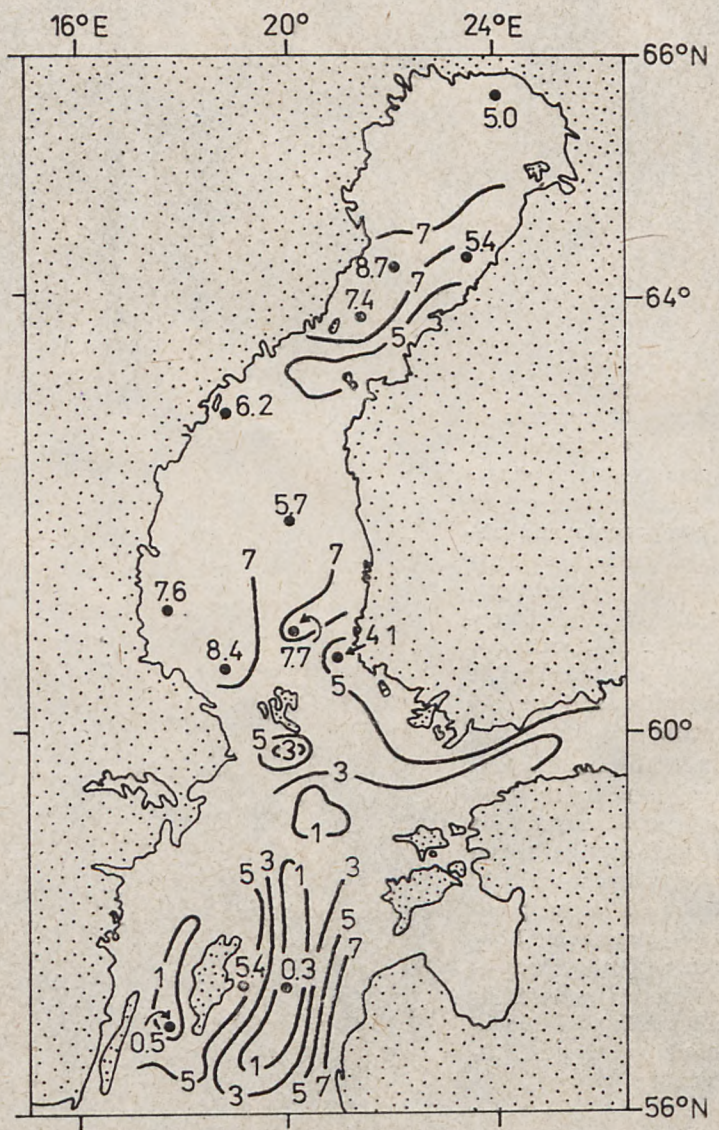

Fig. 14. Oxygen concentration [ml/litre] on the Baltic Sea floor; July — August, 1954 [4]

Rys. 14. Stężenie tlenu [ml/litr] na dnie morza w Bałtyku; lipiec — sierpnień, 1954 [4]

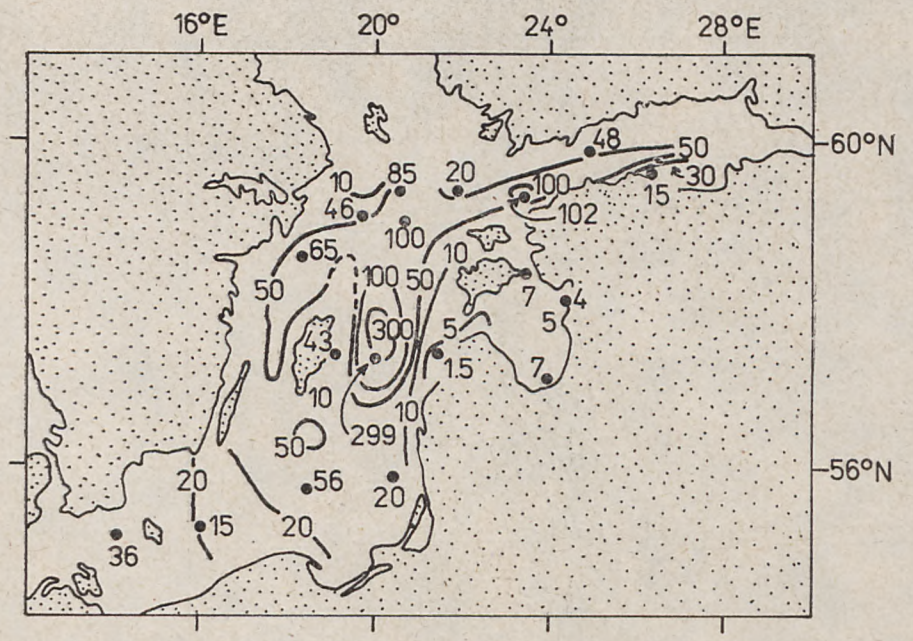

Fig. 15. Phosphate concentration [μg P/litre] on the Baltic Sea floor; August 1960 [4]

Rys. 15. Stężenie fosforanów [μgP/litr] na dnie morza w Bałtyku; sierpień 1960 [4]

the fields of factors which characterize water dynamics and the fields of nutrients. The convergence of the localization of gyres in the mass transport and current fields (Figs. 2, 4, 5) with the areas of high or low concentration of nutrients (Gotland Deep) is obvious. The heterogenity of the water density field and the sea bottom configuration result in the formation of closed circulation systems, characteristic of which is the poor exchange of water with the surrounding areas. The distribution of oxygen, silicates and phosphates in the vicinity of Gotland Deep shown in Figs. 14—16, may be the result of this phenomenon.

Sea bottom currents (Fig. 5) can help in the assessment of the movement of rubble. The mass transport field enables the assessment of water exchange between the Baltic Sea and its bays. As an example we shall give the magnitude of water exchange between the Baltic and the Gulf of Gdańsk (the boundary lies on the line connecting Cape Rozewie and Cape Taran), which amounts to $Q = 1.088 \times 10^{11}\ g\ s^{-1}$. This number characterizes, of course, the steady circulation in the summer season (August).

The author wishes to express his thanks to Prof. dr hab. Zygmunt Kowalik for his scientific supervision during the model investigations and to dr Antoni Staśkiewicz for valuable comments and advice during the computer work.

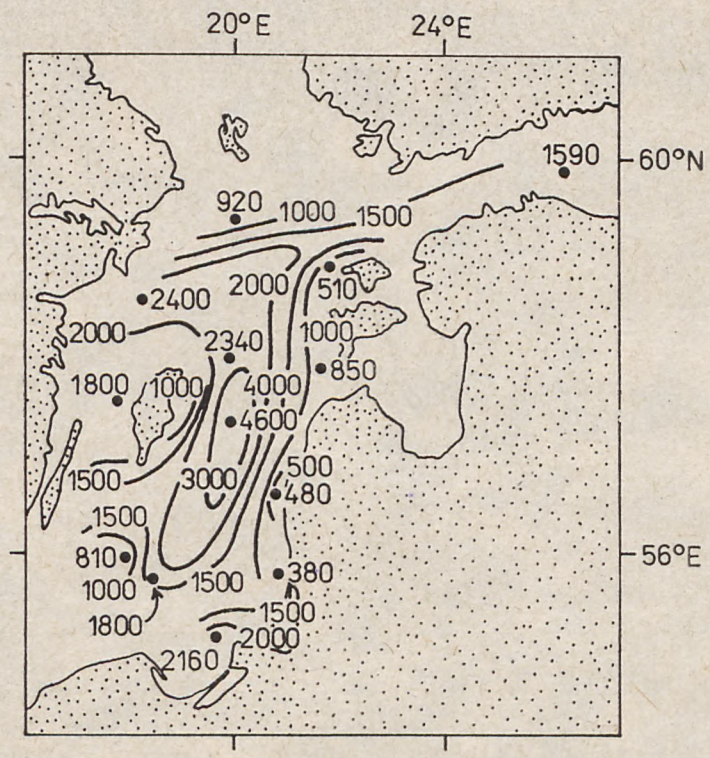

Fig. 16. Silicate concentration [μg Si/litre] on the Baltic Sea floor; August 1958 [4]

Rys. 16. Stężenie krzemianów [μg Si/litr] na dnie morza w Bałtyku; sierpień 1958 [4]

Andrzej JANKOWSKI

Polska Akademia Nauk —
Zakład Oceanologii w Sopocie

MODEL H-N DO OBLICZEŃ USTALONYCH PRZEPŁYWÓW W MORZU BAŁTYCKIM CZĘŚĆ II

Streszczenie

Publikacja niniejsza jest kontynuacją pracy autora omawiającej model hydrodynamiczno-numeryczny (H-N) do badań ustalonych przepływów wiatrowo-gęstościowych w Bałtyku [7]. Obecnie przedstawione są wyniki obliczeń numerycznych ustalonych przepływów gęstościowych dla okresu letniego. Pole gęstości wody opra-

cowano opierając się na metodzie parametryzacji rozkładów pionowych temperatury i zasolenia [8], wyzyskując znane z obserwacji [1, 11] pola temperatury i zasolenia wody w sierpniu.

Rezultaty obliczeń stanowią mapy wydatków masowych, poziomu morza oraz prądów na powierzchni i dnie Bałtyku (rys. 2—5). Pionowe rozkłady składowych prędkości prądu (rys. 7, 8) dopełniają przestrzennego obrazu pola prądów. Profile pionowe temperatury, zasolenia i gęstości wody, przedstawione również na rys. 7 i 8, wskazują na korelację struktury pionowej tych wielkości ze strukturą pionową składowych prędkości prądu.

Spożytkowując wyniki obliczeń przepływów czysto gęstościowych i wiatrowych w morzu jednorodnym [7] dokonano oceny roli obu czynników generujących cyrkulację poziomą wód w Bałtyku (rys. 9—11). Wykazano, że dla silnych wiatrów, o prędkościach $\geqslant 7$—$10\ m\,s^{-1}$, na przeważającym obszarze Morza Bałtyckiego decydujący wpływ na pola wydatków masowych i poziomu morza ma wiatr. W wypadku prądów na powierzchni morza nawet słabe wiatry, o prędkości $\sim 3\ m\,s^{-1}$, wnoszą większy wkład niż gęstość. Jednak w głębszych warstwach morza decydującą rolę odgrywa niejednorodność pola gęstości wody.

Wyniki obliczeń modelowych porównano z rezultatami obserwacji prądów na latarniowcach (rys. 12, tabl. 1 i 2). Wartości prędkości prądów obliczonych i pomierzonych są zbliżone. Większe różnice występują w kierunkach prądów. Na rys. 13 przedstawione są rozkłady pionowe prędkości prądu i gęstości wody zmierzone in situ na Głębi Gdańskiej [2] i obliczone na podstawie modelu H-N. Porównanie wyników pozwala ocenić wpływ rozkładów gęstości wody na strukturę przestrzenną prędkości prądów.

W końcowej części pracy porównano mapy wydatków masowych oraz prądów z rozkładami gęstości wody i substancji biogenicznych na dnie morza (rys. 6, 14—16). Korelacja zawirowań pól wydatków i prądów z obszarami o niskim lub wysokim stężeniu substancji biogenicznych wskazuje na możliwość zastosowania wyników obliczeń modelowych przepływów do oceny przenoszenia substancji biernych w Bałtyku.

REFERENCES

1. Bock, K. H., *Monatskarten des Saltzgehaltes der Ostsee*, Deutsches Hydrographisches Institut, Hamburg 1971, 148.
2. Catewicz, Z., *Zmienność mezoskalowa prądów na Głębi Gdańskiej*, Studia i Materiały Oceanologiczne, nr 26, 1979.
3. Felzenbaum, A. I., *Gidrodinamicheskie modeli neodnorodnogo okeana ili morya*, in: *Problemy teorii vetrovykh i termokhalinnykh techenii*, Izdat. Morskogo Gidrofiz. Inst. AN USRR, Sevastopol' 1968, 29 - 58.
4. Chernovskaya, E. N. [et al.], Gidrometeorologicheskoe Izdat., Leningrad 1965, 168.
5. Hansen, W., *Hydrodynamical methods applied to oceanographical problems*, Proc. Sympos. Mathem.-Hydrodyn. Methods of Phys. Oceanogr., Mitt. Inst. Meeresk. Univ. Hamburg, H. 1, 1962, 25—34.
6. Jankowski, A., *Pewne aspekty zastosowania schematu różnicowego H-N do obliczeń cyrkulacji wiatrowej*, Studia i Materiały Oceanologiczne, nr 16, 1976, 21—38.

7. Jankowski, A., *An H-N model for the calculation of steady wind- and density-driven circulation in the Baltic Sea*, part I: *Theoretical bases. Wind-driven circulation in a homogeneous basin*, Oceanologia, 1983.
8. Jankowski, A., S. Taranowska, *Zastosowanie metody parametryzacji rozkładów pionowych temperatury i zasolenia do opracowania pola gęstości*, Oceanologia, nr 12, 1979.
9. Kowalik, Z., A. Staśkiewicz, *Diagnostic model of the circulation in the Baltic Sea*, Deutsch. Hydrogr. Z., Bd. 29, 1976, H. 6, 239—250.
10. Kowalik, Z., S. Taranowska, *Prądy gęstościowe w Bałtyku*, Oceanologia, nr 3, 1975, 5—31.
11. Lenz, W., *Monatskarten der Temperatur der Ostsee*, Deutsches Hydrographisches Institut, Hamburg 1971, 148.
12. Mamaev, O. I., *T, S — analiz vod mirovogo okeana*, Gidrometeoizdat, Leningrad 1970, 364.
13. Palmen, E., *Untersuchungen über die Stromungen in den Finnland umgebenden Meeren*, Soc. Scient. Fennica, Comentationes Physici—Mathematicae, Vol. 12, 1923, 1—94.
14. Sarkisyan, A. S., *Chislennyi analiz i prognoz morskikh techenii*, Gidrometeoizdat, Leningrad 1977, 184.
15. Sarkisyan, A. S., A. Staśkiewicz, Z. Kowalik, *Diagnosticheskii raschet letnei tsirkulgatsii vod Baltiiskogo morya*, Okeanologia, t. 15, 1975, nr 6, 1002—1009.
16. Simons, T. J., *Topographic and baroclinic circulation in the Southwest Baltic*, Berichte aus dem Inst. Meeresk. Univ. Kiel, H. 25, 1976.
17. Soskin, I. M., *Mnogoletnie izmeneniya gidrologicheskikh kharakteristik Baltiiskogo morya*, Gidrometeorologicheskoe Izdat., Leningrad 1963, 160.
18. Soskin, I. M., L. N. Kuznetsov, V. I. Solovev, *Techeniya Baltiiskogo morya na osnove obratbotki gidrologicheskikh nablyudenii dinamicheskim metodom*, Trudy Gosud. Okeanogr. Inst., t. 73, 1963, 76—95.
19. Vasilev, A. S., *O primenenii modelei plotnosti, temperatury i solonosti v teorii okeanicheskikh techenii*, in: *Problemy teorii vetrovykh i termokhalinnykh techenii*, Izdat. Morskogo Gidrofiz. Inst. AN USRR, Sevastopol 1968, 168—181.